Journal of the Mechanical Behavior of Biomedical Materials 78 (2018) 108–115

Contents lists available at ScienceDirect

Journal of the Mechanical Behavior of Biomedical Materials

journal homepage: www.elsevier.com/locate/jmbbm

Location-specific mechanical response and morphology of facial soft tissues

Marco Pensalfini[a,*], Johannes Weickenmeier[a,b], Marga Rominger[c], Roberto Santoprete[d], Oliver Distler[e], Edoardo Mazza[a,f]

[a] Institute for Mechanical Systems, Department of Mechanical and Process Engineering, ETH Zurich, Leonhardstrasse 21, 8092 Zurich, Switzerland
[b] Department of Mechanical Engineering, Stanford University, Stanford, CA 94305, USA
[c] Institute for Diagnostics and Interventional Radiology, University Hospital Zurich, Rämistrasse 100, 8091 Zurich, Switzerland
[d] L'Oréal Research & Innovation, Avenue Eugène Schueller 1, 93601 Aulnay-sous-Bois, France
[e] Department of Rheumatology, University Hospital Zurich, Rämistrasse 100, 8091 Zurich, Switzerland
[f] Empa, Swiss Federal Laboratories for Materials Science and Technology, Überlandstrasse 129, 8600 Dübendorf, Switzerland

ARTICLE INFO

Keywords:
Facial skin biomechanical characterization
Suction-based measurements
Location-specific characterization
Suction method repeatability
Skin layer morphology
High frequency ultrasounds

ABSTRACT

The facial tissue of 9 healthy volunteers (m/f; age: 23–60 y) is characterized at three different locations using a procedure combining suction measurements and 18 MHz ultrasound imaging. The time-dependent and multi-layered nature of skin is accounted for by adopting multiple loading protocols which differ with respect to suction probe opening size and rate of tissue deformation. Over 700 suction measurements were conducted and analyzed according to location-specific mechanical and morphological characteristics. All corresponding data are reported and made available for facial tissue analysis and biomechanical modeling. Higher skin stiffness is measured at the forehead in comparison to jaw and parotid; these two regions are further characterized by lower creep deformation. Thicker tissue regions display a tendency towards a more compliant and less dissipative response. Comparison of superficial layer thickness and corresponding mechanical measurements suggests that connective tissue density determines the resistance to deformation in suction experiments.

1. Introduction

Realistic representation of the mechanical behavior of facial skin for surgical planning (Chabanas et al., 2003; Mollemans et al., 2007; Chabanas and Payan, 2000; Pieper et al., 1995; Beldie et al., 2010), virtual reality and animation rendering (Beldie et al., 2010), as well as aging simulations (Barbarino et al., 2009) requires biophysically-motivated numerical models. In this context, understanding the regional differences of mechanical behavior within the face sets the basis for enhanced model accuracy. In particular, more realistic simulations can be obtained using models that account for variation of mechanical parameters in different regions of the face.

It is well understood that the mechanical and morphological characteristics of soft tissues depend on gender (Luebberding et al., 2014; Cua et al., 1990; Diridollou et al., 2000; Weickenmeier et al., 2015), body location (Luebberding et al., 2014; Cua et al., 1990; Diridollou et al., 2000; Weickenmeier et al., 2015; Couturaud et al., 1995; Luboz et al., 2014; Ryu et al., 2008; Smalls et al., 2006; Krueger et al., 2011; Takema et al., 1994; Maibach, 2002), and age (Luebberding et al., 2014; Cua et al., 1990; Couturaud et al., 1995; Ryu et al., 2008; Krueger et al., 2011; Takema et al., 1994; Staloff et al., 2008; de Rigal et al., 1989). Cosmetic industries (Barbarino et al., 2009; Then et al., 2017) and clinicians (Luboz et al., 2005) share an interest in predictive tools capable of describing subject-specific changes in the appearance of the face and associated mechanical properties. Corresponding skin models must account for tissue properties across multiple length-scales and incorporate the mechanical interactions between individual superficial layers. Most investigations on skin biophysics use the aspiration technique – first presented in the 1970s by Grahame (1970) and Alexander and Cook (1977) – to measure the *in vivo* mechanical behavior of the tissue. The working principle is based on the application of a negative pressure to the skin surface by means of a suction cup; the same tool is used to measure the corresponding tissue elevation. The two most common commercial systems are the Dermaflex A (Cortex Technology, Hadsund, Denmark) and the Cutometer® (Courage + Khazaka, Cologne, Germany); both characterize the complex nonlinear and time-dependent response of the superficial skin layers by controlling the level of pressure applied. Given its simple applicability, the suction technique has been used to study the mechanical characteristics of skin under the influence of age (Luebberding et al., 2014; Cua et al., 1990; Diridollou et al., 2000; Couturaud et al., 1995; Ryu et al., 2008; Krueger et al., 2011; Takema et al., 1994), gender (Luebberding et al., 2014; Cua et al.,

* Corresponding author.
E-mail address: marcopen@ethz.ch (M. Pensalfini).

https://doi.org/10.1016/j.jmbbm.2017.10.021
Received 10 July 2017; Accepted 16 October 2017
Available online 14 November 2017

1990; Diridollou et al., 2000), and body location (Luebberding et al., 2014; Cua et al., 1990; Diridollou et al., 2000; Couturaud et al., 1995; Ryu et al., 2008; Smalls et al., 2006; Krueger et al., 2011; Takema et al., 1994; Maibach, 2002), as well as the effect of hydration (Maibach, 2002; Murray and Wickett, 1996; Dobrev, 2000), wounds (Fong et al., 1997; van Zuijlen et al., 2000; Rennekampff et al., 2006; Moiemen et al., 2011), and cutaneous diseases (Maibach, 2002; Piérard et al., 2013; Dobrev, 2013). The well-defined boundary conditions provided by this method have promoted the use of suction measurements to calibrate numerical models (Weickenmeier et al., 2015; Luboz et al., 2005; Barbarino et al., 2011; Weickenmeier and Jabareen, 2014). Most of the *in vivo* studies on skin rely on the Cutometer®, which allows to recruit different tissue layers by varying the probe opening diameter; the measurement outcome is expressed *via* a set of parameters directly computed by the provided software interface.

Varying properties have been reported for different facial regions, in association with different morphological and functional tissue characteristics (Ghassemi et al., 2003). With particular reference to the face, Weickenmeier et al. (2015) measured a similar mechanical response for the forehead and parotidomasseteric regions in a single-subject study, whereas they found the jaw tissue to be softer. Most studies in the literature focus on the most superficial skin layers, whose mechanical response under suction is typically considered to be dominated by the dermal characteristics. Fewer investigations (Weickenmeier et al., 2015; Hendriks et al., 2003; Diridollou et al., 1998; Vogt and Ermert, 2005) included information from the underlying subcutaneous fat and observed a dominant role of the dermis over the subcutis, as the former is richer in collagen fibers (Agache, 2004). Nonetheless, these works also showed an influence of the fat layer in the deformation process of the skin, possibly contributing to the inelastic properties measured with relatively large probe openings. The biophysical characteristics of this deep tissue remain poorly investigated. Understanding its role in terms of *in vivo* mechanics is crucial to establish models that are able to accurately reproduce facial expressions, as this layer represents the intermediate structure between the activated muscles and the skin. Additionally, the septae located at the subcutaneous fat level have been suggested to play a role in defining possible aging patterns (Ezure et al., 2009).

The present work is based on three main hypotheses:

H1. The skin response to ramp and step suction loadings varies significantly between the different regions of the face; this investigation focuses on the tissue layers located in the forehead, parotid, and jaw.

H2. Different regions are also characterized by different thicknesses of these layers.

H3. The *in vivo* mechanical characteristics correlate with layer thicknesses.

Over 700 suction measurements were performed on nine volunteers of different age and gender with a protocol focusing on controlled positioning of the probe and including a wide range of step and ramp loading conditions. High resolution ultrasound measurements were performed at the same location of suction measurements in order to quantify the thickness of several visible tissue layers.

2. Methods

2.1. Volunteer recruitment

The present study was approved by the ETH Zurich ethic commission (EK 2015-N-63) and involved nine individuals: 3 young men (23 ± 1 y), 3 young women (24 ± 2 y), and 3 senior women (57 ± 3 y); all were recruited from a pool of subjects who had participated in an investigation on skin elastography performed at the University Hospital Zurich (KEK-ZH 2015-0323) and provided written informed consent for acquisition of the data and their use for scientific purposes. Measurements were performed at ETH Zurich (suction) and at the University Hospital Zurich (US imaging).

2.2. Testing rig

The custom-modified headrest, presented in (Weickenmeier et al., 2015), allows to control the contact pressure between the probe and the subject and to ensure repeatable probe placement at multiple facial locations. Measurements are carried out using the Cutometer® MPA 580 (Courage + Khazaka, Cologne, Germany) and two suction probes with opening diameters of 2 and 8 mm. This provides enhanced control over the specific recruitment of cutis and subcutis in individual measurements. The accompanying Cutometer® MPA Q software controls the prescribed suction protocol and automatically determines a set of predefined parameters after each measurement (cf. Section 2.3). All parts of the rig in contact with the subject's skin are thoroughly disinfected before and after each measurement session.

2.3. Loading protocols and parameters

To determine the skin tissue response under various loading conditions, ten different loading protocols are defined (Table 1). Fast application of the negative pressure (step) reveals the instantaneous and creep behavior of the tissue, while continuous loading and unloading protocols (ramp) capture the transient tissue behavior. Every protocol is repeated 3–4 times in each of the three facial locations considered for this study (Weickenmeier et al., 2015; Barbarino et al., 2011), namely forehead, parotid, and jaw. These regions are selected based on anatomical considerations with respect to local tissue composition, layer thickness, and tissue layer interaction. Based on previous work (Weickenmeier et al., 2015), 30–45 s resting intervals are prescribed between each measurement to ensure tissue recovery. An analysis of the preconditioning effects possibly induced by repeated loadings is reported in the Supplementary material and shows that the interval between measurements is sufficiently long to allow for tissue recovery.

For both step and ramp loading modes, two of the 19 parameters provided by the Cutometer® software are selected (Fig. 1). In case of rapid loading (Mode 1 (Courage + Khazaka Electronic GmbH, 2010)), the parameters U_e and R6 are adopted. The former describes the instantaneous elastic tissue response in terms of its elevation after 0.1 s from the instant of first load application, and it is expressed in mm; the latter is a measure for the subsequent creep response during the hold period at maximum pressure. U_e is obtained based on the values provided by the software for R7, R0, and R5: $U_e = R7 \cdot R0/R5$ (Courage + Khazaka Electronic GmbH, 2010). In case of continuous loading and unloading (Mode 2 (Courage + Khazaka Electronic GmbH, 2010)), the elevation at maximum pressure, R0 (expressed in mm), and the

Table 1
Definition of the test parameters according to the Cutometer® MPA Q software. Ten different loading protocols were considered in the study; they differ in terms of deformation rate, loading magnitude, and probe opening size. Denominations are as per (Courage + Khazaka Electronic GmbH, 2010).

Protocol Name	Opening Ø [mm]	Mode [-]	On-time [s]	Pressure [mbar]	Off-time [s]
2S300	2	1	60.0	300	0.1
2S500	2	1	60.0	500	0.1
8S66	8	1	30.0	66	0.1
8S133	8	1	30.0	133	0.1
8S200	8	1	30.0	200	0.1
2R10	2	2	17.5	175	0.1
2R15	2	2	17.5	263	0.1
8R10	8	2	10.0	100	0.1
8R15	8	2	10.0	150	0.1
8R20	8	2	10.0	200	0.1

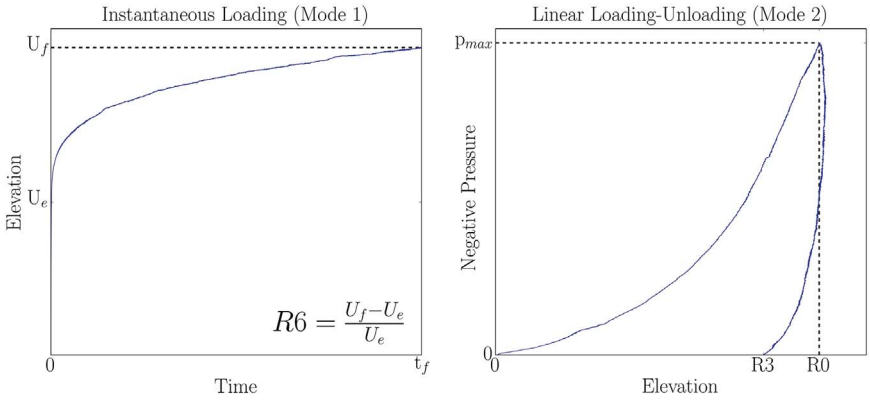

Parameter	Tissue Behavior of Interest
U_e	Instantaneous compliance
R6	Creep response

Parameter	Tissue Behavior of Interest
R0	Time-dependent compliance
R3/R0	Inelastic response

Fig. 1. Exemplification of the applied loading modes. The quantities useful for the definition of the parameters used to express the outcome of the suction measurements are indicated; the mechanistic interpretation of the chosen parameters is also explained.

residual-to-maximum pressure elevation ratio, R3/R0, are selected to describe the time-dependent tissue compliance and inelastic response.

2.4. Thickness measurements

Skin thickness measurements are based on B-mode high resolution (~ 30 μm/pixel) ultrasound imaging. Three images are acquired at each facial location using an 18 MHz hockey-stick probe on a LOGIQ E9 (GE Medical Systems, Glattbrugg, Switzerland) machine available at the University Hospital. A SonarAid (Geistlich Pharma AG, Wolhusen, Switzerland) Ultrasound Gel Pad is placed between the probe and the skin to enhance acoustic impedance coupling. The individual, visually differentiable tissue layers are manually segmented in each ultrasound image using a custom-written Python code (Python Software Foundation) to calculate the respective thickness (de Rigal et al., 1989; Laurent et al., 2007). Given the echogenicity of full-thickness skin, four tissue layers can be differentiated: epidermis, subepidermal low echogenic band (SLEB, roughly corresponding to papillary dermis), dermal echogenic band (DEB, roughly corresponding to reticular dermis), and the subcutis (Fig. 2). The cutis is comprised of the epidermis and dermis. The latter may be further differentiated into SLEB and DEB, as per Laurent et al. (2007) and Wortsman et al. (2013). In the present study, epidermis and SLEB are considered as a single layer (ESLEB) due to a limited resolution of the most superficial layer thickness using the chosen ultrasound system.

2.5. Statistical analysis

Correlation of suction data with skin layer thicknesses is assessed *via* Spearman's test. The Python function “stats.spearmanr” available within the SciPy library (Python Software Foundation) is used to this end.

In the interest of robustness with respect to outliers, the following definition is considered for the coefficient of variation: $CV = MADM/m$. $MADM$ is the median absolute deviation from the median and m the median of the distribution.

Statistical significance of the observed differences is assessed *via* Kruskal-Wallis H test with Tukey-Cramer post-hoc test; the level of significance is set to $p < 0.05$. The Matlab (Mathworks Inc., Natick, MA, USA) functions “kruskalwallis” and “multcompare” are used to perform the Kruskal-Wallis and post-hoc tests, respectively. Note that the use of a non-parametric method does not require to assume that the data are drawn from a normal distribution.

3. Results

3.1. Repeatability of suction data

Tissue recovery between repeated loading (see Supplementary material) allows each measurement to be considered as an independent event. The variability of the suction method is thus assessed by comparing results obtained from nominally identical measurements, *i.e.* when considering the same loading protocol, location, and subject. The median coefficient of variation for each probe opening and Cutometer® parameter is reported in Table 2. With the exception of R6, this analysis reveals a setup ensuring excellent measurement repeatability. The 8 mm probe is found to yield slightly more repeatable observations than the 2 mm one; R6 constitutes an exception also in this sense.

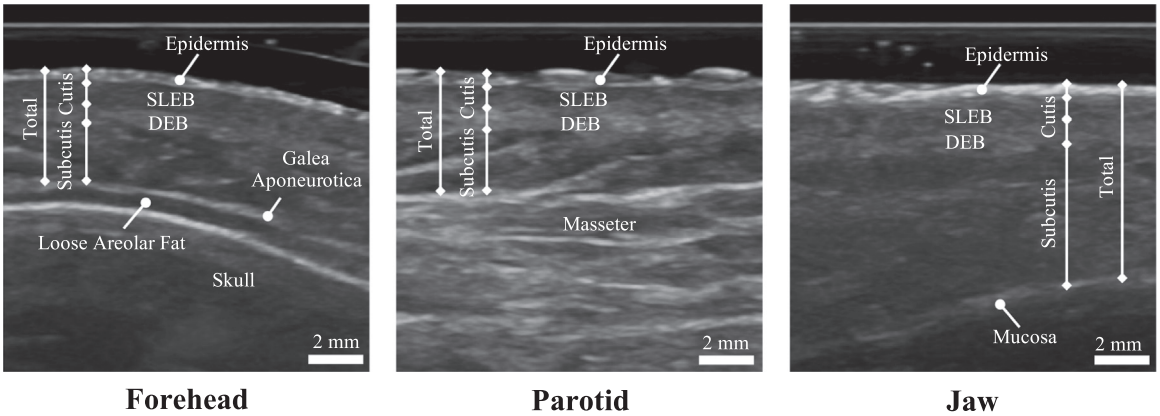

Fig. 2. Definition of the tissue layers as measured in the ultrasound images at each of the considered facial locations. The cutis results from associating epidermis, SLEB, and DEB together.

Table 2
Median variability for each probe opening and considered parameter.

Measurement Variability	Ramp Load - R0		Ramp Load - R3/R0		Step Load - U_e		Step Load – R6	
Opening Diameter	**2 mm**	**8 mm**	**2 mm**	**8 mm**	**2 mm**	**8 mm**	**2 mm**	**8 mm**
Coefficient of Variation [%]	3.0	1.9	3.6	3.3	4.4	3.4	7.5	11.0
Sample Size [-]	44	52	44	52	45	51	45	51

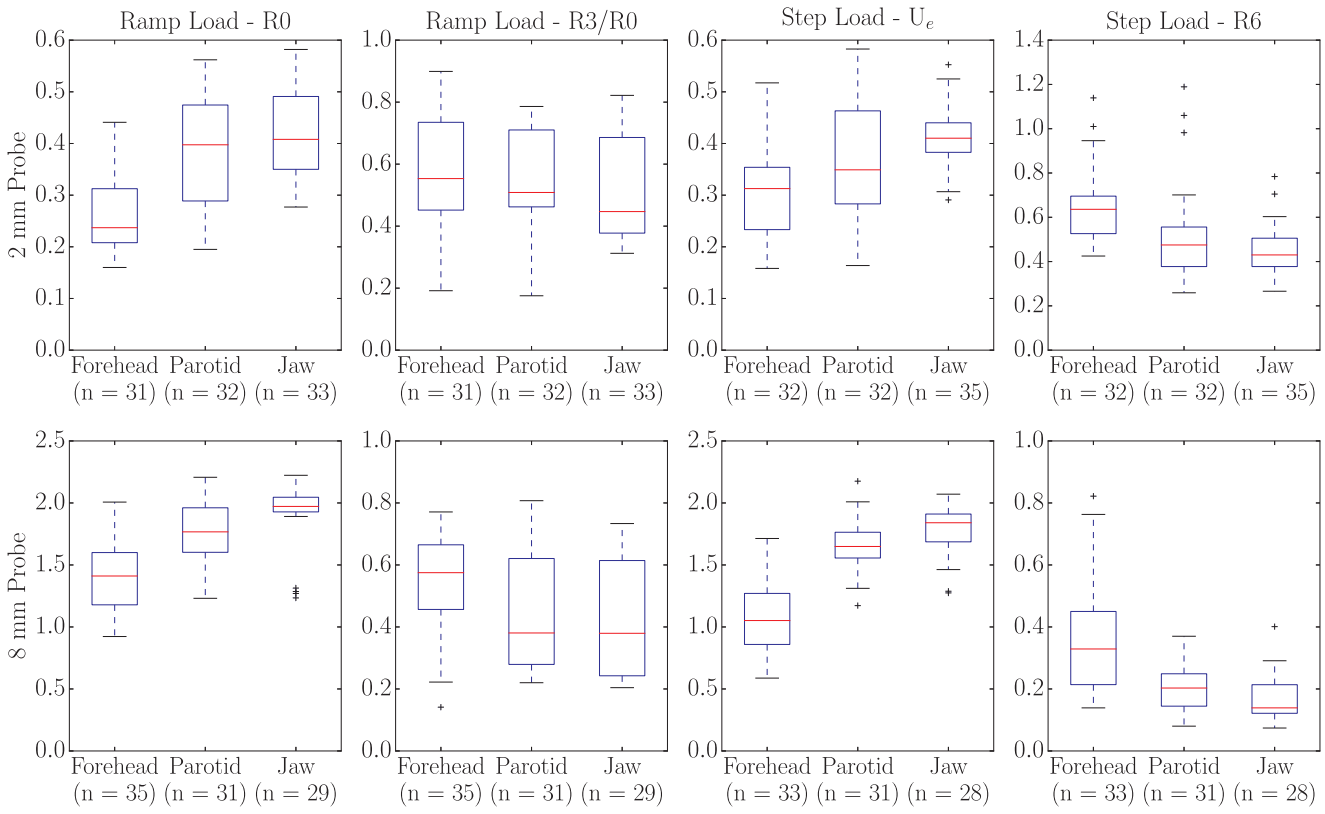

Fig. 3. Comparison of facial locations in terms of measured suction parameters. The general trends show decreasing stiffness and dissipative features when moving from the forehead to the parotid and jaw.

3.2. Location-specific mechanical characteristics

Further analysis is carried out on a subset of four loading protocols, *i.e.* 2R15, 2S500, 8R15, and 8R133 (cf. Table 1), for which data could be consistently collected from all nine volunteers. The whole dataset of this experimental campaign is reported in the Supplementary material.

Fig. 3 shows the distribution of data for different facial locations, suction probe openings, and measured parameters in terms of boxplots, while Table 3 summarizes the outcome of statistical comparisons (Kruskal-Wallis H test with Tukey-Cramer post-hoc test; $p < 0.05$). The forehead is found to differ significantly from both parotid and jaw. The largest differences are observed between forehead and jaw, where the median value of R0 varies by up to 40% (2 mm probe), along with an 8 mm U_e that is 43% larger for the jaw than for the forehead and 2 mm U_e values that differ by a more modest 24%. Strikingly, the values of the dissipative parameter R3/R0 are rather consistent across the study, not only among locations but also between the two different probes. The only determined significant difference corresponds to measurements involving the deeper tissues of forehead and jaw (8 mm opening), the latter being 52% more elastic than the former. Conversely, R6 shows clear location specificity for both probes, with the largest differences occurring once again for the comparison between the 8 mm measurements performed on the forehead and jaw (137% variation). These results confirm hypothesis H1 of the present study.

Table 3
Summary of the statistically significant results found when comparing the outcome of suction measurements performed at different facial locations (Kruskal-Wallis H test with Tukey-Cramer post-hoc test; $p < 0.05$).

Loading mode	Parameter	Probe	
		2 mm	**8 mm**
Ramp	**R0**	F < P	F < P
		F < J	F < J
	R3/R0	–	F > J
Step	**U_e**	F < P	F < P
		F < J	F < J
	R6	F > P	F > P
		F > J	F > J

3.3. Location-specific skin layer thicknesses

The measured layer thicknesses are compared across locations (Fig. 4; individual values are reported in the Supplementary material). Interestingly, cutis, subcutis, and the entire skin are significantly thinner in the forehead and parotid in comparison to the jaw (Kruskal-Wallis H test with Tukey-Cramer post-hoc test; $p < 0.05$), which contrasts the outcome of suction measurements. Median thickness values differ by 12–13% at the cutis level, by 67–71% at the subcutis level, and by 52–55% at the whole thickness level. Besides, the ESLEB thickness

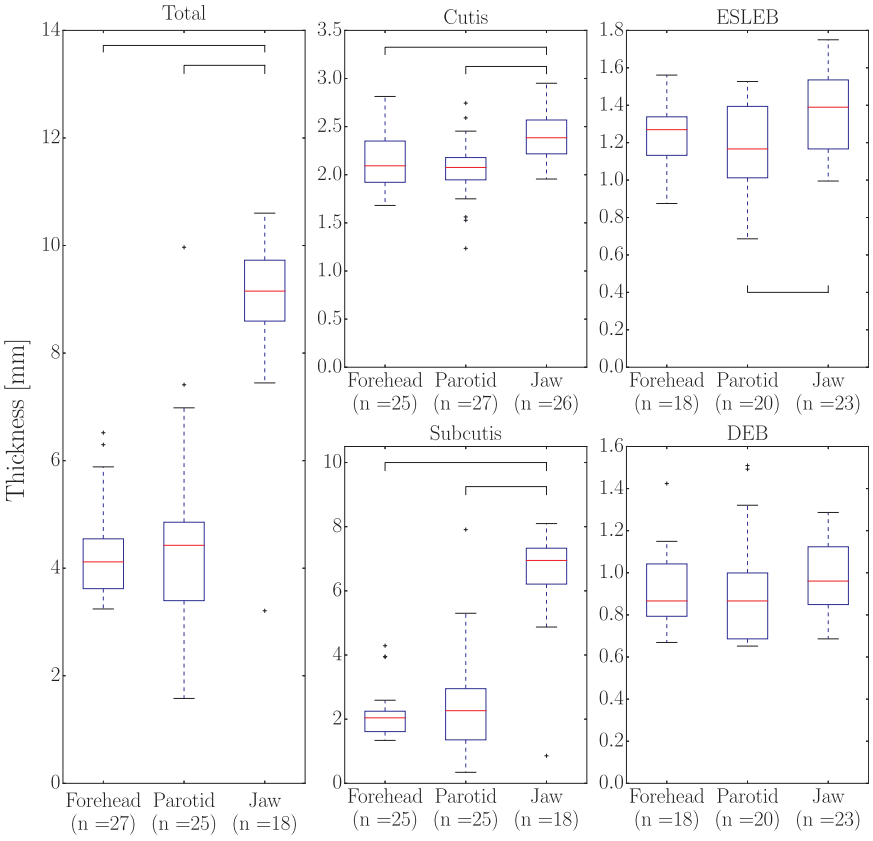

Fig. 4. Comparison of facial locations in terms of skin layer thicknesses according to the distinction defined in Section 2.4. Statistically significant differences are indicated on the chart and only occur between jaw and forehead or parotid (Kruskal-Wallis H test with Tukey-Cramer post-hoc test, $p < 0.05$).

also differs significantly between parotid and jaw (16% larger in the latter). It is worth noting that the ESLEB and DEB thickness are generally comparable for all considered locations, while the cutis is much thinner than the subcutis in the jaw region; this is possibly associated with the absence of underlying structures such as bones or muscles, which are instead present in the forehead and parotid regions. Taken together, these data confirm hypothesis H2.

3.4. Relation between layer thickness and suction response

The relation between layer thicknesses and Cutometer® parameters is investigated via Spearman's correlation test. Fig. 5 shows the average of repeated measurements per location and subject, as well as the rank-order coefficient (ρ) and p value obtained for each correlation. Only the comparisons yielding $p < 0.05$ are reported in Fig. 5; note that Spearman's test investigates monotonicity and not linearity.

Positive correlations ($\rho \cong 0.5$) are identified between the 2 mm R0 and U_e parameters and the ESLEB thickness (Fig. 5a-b), as well as between the 8 mm R0 and the subcutis and whole tissue thicknesses (Fig. 5e-f). A similar tendency is also present for the relation between the 8 mm R0 and the ESLEB thickness, which appears to approach significance ($p = 0.06$; not shown). At the same time, the inelastic parameters show decreasing trends for increasing thickness: R3/R0 correlates negatively with the ESLEB thickness for both probe openings ($\rho \cong -0.5$; Fig. 5c-d), while the 8 mm R6 correlates negatively with the subcutis and total thickness ($\rho \cong -0.4$; Fig. 5g-h).

While these results confirm the existence of correlations between suction parameters and skin layers thickness (hypothesis H3), the fact that thinner tissues oppose stronger resistance to suction deformation is contrary to our initial expectation.

4. Discussion

4.1. Methodological considerations

The adopted experimental setup addresses one of the primary limitations of suction measurements, namely the difficulty to achieve good repeatability associated with manual holding of the probe by the operator. This is achieved by using a rig that allows for flexible and reproducible alignment of the probe with respect to the subject. The coefficient of variation related to nominally identical measurements was quantified and showed median values in the range of 2–5% (Table 2), except for R6 for which a larger scatter of 8–11% was observed. In spite of the complexity associated with performing measurements on the human face, these values are low and comparable with those previously reported for measurements performed on the volar forearm (Piérard et al., 1995; Jemec et al., 1996) – a location for which probe positioning is less affected by relative movements. Note that Piérard et al. (1995) also found a larger variability when measuring R6 as compared to U_e. This might be due to the lack of tissue guidance during the creep phase, which is associated with the constant pressure level imposed, as opposed to an increasing or decreasing load associated with each one of the other parameters measured in this study.

The adopted testing rig offers several advantageous features: it reduces the need for operator training, it reduces their interaction with the probe during testing, and it allows repeatable repositioning of the probe and stable contact conditions during experiments.

4.2. Distinctive features of facial locations

The results reported in Fig. 3 and Table 3 confirm systematic differences in tissue characteristics between facial locations. They suggest that the forehead is consistently the stiffest and most dissipative of all considered regions. Parametric variations of the constitutive coefficients in axisymmetric finite element models incorporating the

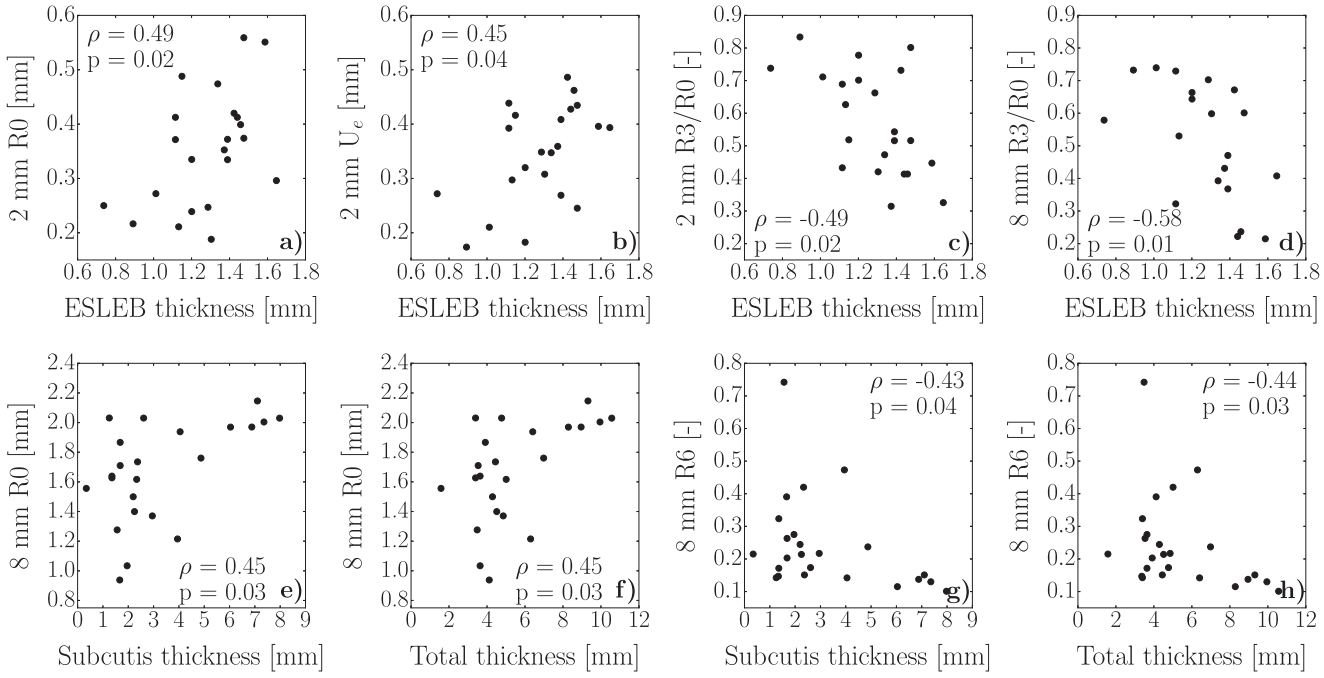

Fig. 5. Comparison between mechanical characteristics and thickness of several tissue layers. The elastic parameters (R0 and U_e; a,b,e,f) correlate positively with the thickness, while the inelastic ones show negative trends (c,d,g,h).

multilayered structure of facial tissues (data not shown) indicate that this can be mainly attributed to the characteristics of the cutis, which is often considered the mechanically dominant layer, see *e.g.* Vogt and Ermert (2005). Previous studies also reported a stiff forehead when compared to the cheek region (which might be expected to be similar to the jaw) (Takema et al., 1994; Barbarino et al., 2011), while Luboz et al. (2014) reported lower stiffness for the forehead than for cheek and lower lip areas. However, their use of a probe with an opening diameter of 12 mm is likely to affect the initial elevation of the skin and might influence the overall measurement results, especially when comparing different facial locations.

4.3. Layer-specific dissipative characteristics

In contrast to most skin studies found in the literature, which rely on the use of a creep test-like (step) loading mode, the present work applied an additional ramp-like protocol. This, in combination with different suction areas, allows characterizing the transient properties of the individual layers and thus accounting for their complex time-dependent mechanical behavior (Weickenmeier et al., 2015; Piérard et al., 2013). The determined values of R3/R0 are comparable for both probe openings, suggesting a common mechanism of elastic tissue recovery. Conversely, the R6 values are larger for the 2 mm than for the 8 mm probe, which indicates different processes for tissue creep. This might be associated with the subcutis contribution to the instantaneous response of the 8 mm probe, as well as with the different deformation modes induced by the two probe openings in the superficial skin layer. In particular, as supported by finite element simulations based on the modeling approach introduced in (Weickenmeier et al., 2015; Weickenmeier and Jabareen, 2014), the 2 mm probe primarily applies a localized lifting and shear deformation to the cutis, which is possibly associated with more pronounced transient effects, while the 8 mm probe results in global bending and stretching, which causes the subcutaneous fat to rapidly move towards the region of load application.

4.4. Role of tissue layer thickness

For both cutis and subcutis regional differences in thickness were confirmed. However, in contrast to the suction measurements, layer thicknesses were not found to differ significantly between forehead and parotid, but much so when comparing each of these two regions with the jaw (Fig. 4).

The determined correlation between mechanical and morphological measurements indicates that thinner tissues provide stronger resistance to suction-induced deformation (Fig. 5). In this context, the influence of the subcutis, which constitutes the softest layer, might be associated with the presence of an anchoring point at its lower extremity that, for thicker tissues, is located at larger distances from the region of load application. This might justify the increased tissue compliance when measuring with the 8 mm probe (Fig. 5d,f). On the contrary, the relation between the ESLEB thickness and the elastic parameters obtained with the smaller probe (Fig. 5a,b) is in complete contrast to what would be expected for a homogeneous continuum. This indicates that the discrete, network-like architecture of the dermis plays a dominant role in defining the *in vivo* mechanical behavior of the whole skin, and suggests that the superficial layer thickness might be linked to the density of the load-bearing components of the extracellular matrix (mainly collagen), with thinner cutes corresponding to higher density of collagen fibers, thus yielding stiffer behavior. These results are in line with previous findings from compression tests on murine skin (Wang et al., 2013) and indicate that the normalization of Cutometer® parameters by layer thickness proposed in previous publications (Krueger et al., 2011; Takema et al., 1994; Dobrev, 2000; Edwards et al., 2001) might not be adequate towards a mechanical characterization of the tissue. In fact, the simple proportional relation underlying this normalization would largely overestimate the actual dependence of tissue compliance on its thickness (Fig. 5), besides yielding parameters possessing little mechanical relevance (elevation per unit thickness).

Conversely, the inelastic parameters show decreasing trends as the thickness of ESLEB, subcutis, and of the whole tissue increase. This might be related to increased fibers interaction and entanglement, which are likely to characterize tissues with a denser collagen network, thus leading to a larger rate of non-recoverable deformation (R3/R0). The lower creep compliance (R6) observed for thicker subcutes is again possibly associated with the increased distance between skin surface and fat anchoring point, suggesting quicker reallocation of the

subcutaneous tissue in response to the applied load. Different ways of triggering fluid and tissue motion mechanisms might also be one of the factors contributing to the differences observed when applying different deformation modes and suction probe openings (see Fig. 3 and Section 4.3), particularly at fast loading rates.

5. Conclusions

The present work confirms the location specificity of facial tissue mechanical response, in association with different physiological functions and morphological characteristics. Application of an accurate measurement procedure shows that skin is stiffer, and reveals a more pronounced creep behavior in the forehead in comparison to the parotid and jaw. The expectation that thicker skin correlates with stiffer tissue is not confirmed, suggesting that the compaction of collagen fibers and fluid-motion mechanisms play a primary role.

The present data contribute to a better understanding of *in vivo* skin biomechanics and might be used to inform the development and benchmarking of multilayer regional biomechanical models of the human face.

Acknowledgments

The authors thank the volunteers for their participation in the study and Mattia Bellini for his support during data acquisition. Insightful discussions with Christiane Uhl from Courage + Khazaka Electronic GmbH regarding the use of the Cutometer® MPA 580 and corresponding software are gratefully acknowledged.

This work was conducted as part of the SKINTEGRITY flagship project of University Medicine Zurich (http://www.hochschulmedizin.uzh.ch/en/projekte/skintegrity.html).

Appendix A. Supporting information

Supplementary data associated with this article can be found in the online version at http://dx.doi.org/10.1016/j.jmbbm.2017.10.021.

References

Agache, P., 2004. Dermis. In: Agache, P., Humbert, P. (Eds.), Measuring the Skin. Springer-Verlag, Berlin Heidelberg, pp. 197–203.

Alexander, H., Cook, T.H., 1977. Accounting for natural tension in the mechanical testing of human skin. J. Invest. Dermatol. 69 (3), 310–314.

Barbarino, G.G., Jabareen, M., Trzewik, J., Nkengne, A., Stamatas, G., Mazza, E., 2009. Development and validation of a three-dimensional finite element model of the face. J. Biomech. Eng. 131 (4), 041006-1–041006-11.

Barbarino, G.G., Jabareen, M., Mazza, E., 2011. Experimental and numerical study on the mechanical behavior of the superficial layers of the face. Skin. Res. Technol. 17 (4), 434–444.

Beldie, L., Walker, B., Lu, Y., Richmond, S., Middleton, J., 2010. Finite element modelling of maxillofacial surgery and facial expressions – a preliminary study. Int. J. Med. Robot. Comput. Assist. Surg. 6 (4), 422–430.

Chabanas, M., Payan, Y., 2000. A 3D Finite Element Model of the Face for Simulation in Plastic and Maxillo-Facial Surgery, in Medical Image Computing and Computer-Assisted Intervention – MICCAI 2000. Lecture Notes in Computer Science, Berlin, Heidelberg.

Chabanas, M., Luboz, V., Payan, Y., 2003. Patient specific finite element model of the face soft tissues for computer-assisted maxillofacial surgery. Med. Image Anal. 7 (2), 151–171.

Courage + Khazaka Electronic GmbH, 2010. "Information and Operating Instructions for the Cutometer(R) MPA 580 and the software Cutometer(R) MPA Q, Courage + Khazaka Electronic GmbH, Koeln, Germany.

Couturaud, V., Coutable, J., Khaiat, A., 1995. Skin biomechanical properties: in vivo evaluation of influence of age and body site by a non-invasive method. Skin. Res. Technol. 1 (2), 68–73.

Cua, A.B., Wilhelm, K.-P., Maibach, H.I., 1990. Elastic properties of human skin: relation to age, sex, and anatomical region. Arch. Dermatol. Res. 282 (5), 283–288.

Diridollou, S., Berson, M., Vabre, V., Black, D., Karlsson, B., Auriol, F., Gregoire, J.M., Yvon, C., Vaillant, L., Gall, Y., Patat, F., 1998. An in vivo method for measuring the mechanical properties of the skin using ultrasounds. Ultrasound Med. Biol. 24 (2), 215–224.

Diridollou, S., Black, D., Lagarde, J.M., Gall, Y., Berson, M., Vabre, V., Patat, F., Vaillant, L., 2000. Sex- and site-dependent variations in the thickness and mechanical properties of human skin in vivo. Skin. Res. Technol. 22 (6), 421–435.

Dobrev, H., 2000. Use of cutometer to assess epidermal hydration. Skin Res. Technol. 6 (4), 239–244.

Dobrev, H., 2013. Novel ideas: the increased skin viscoelasticity – a possible new fifth sign for the very early diagnosis of systemic sclerosis. Curr. Dermatol. Rev. 9 (4), 261–267.

Edwards, C., Pearse, A., Marks, R., Nishimori, Y., Matsumoto, K., Kawai, M., 2001. Degenerative alterations of dermal collagen fiber bundles in photodamaged human skin and uv-irradiated hairless mouse skin: possible effect on decreasing skin mechanical properties and appearance of wrinkles. J. Invest. Dermatol. 117 (6), 1458–1463.

Ezure, T., Hosoi, J., Amano, S., Tsuchiya, T., 2009. Sagging of the cheek is related to skin elasticity, fat mass and mimetic muscle function. Skin. Res. Technol. 15 (3), 299–305.

Fong, S.S., Hung, L.K., Cheng, J.C., 1997. The cutometer and ultrasonography in the assessment of postburn hypertrophic scar – a preliminary study. Burns 23 (1), S12–S18.

Ghassemi, A., Prescher, A., Riediger, D., Axer, H., 2003. Anatomy of the SMAS revisited. Aesthetic Plast. Surg. 27 (4), 258–264.

Grahame, R., 1970. A method for measuring human skin elasticity in vivo with observations on the effects of age, sex and pregnancy. Clin. Sci. 39, 223–238.

Hendriks, F.M., Brokken, D., van Eemeren, J.T.W.M., Oomens, C.W.J., Baaijens, F.P.T., Horsten, J.B.A.M., 2003. A numerical-experimental method to characterize the non-linear mechanical behaviour of human skin. Skin. Res. Technol. 9, 274–283.

Jemec, G.B., Gniadecka, M., Jemec, B., 1996. Measurement of skin mechanics. Skin. Res. Technol. 2 (4), 164–166.

Krueger, N., Luebberding, S., Oltmer, M., Streker, M., Kerscher, M., 2011. Age-related changes in skin mechanical properties: a quantitative evaluation of 120 female subjects. Skin. Res. Technol. 17 (2), 141–148.

Laurent, A., Mistretta, F., Bottigioli, D., Dahel, K., Goujon, C., Nicolas, J.F., Hennino, A., Laurent, P.E., 2007. Echographic measurement of skin thickness in adults by high frequency ultrasounds to assess the appropriate microneedle lenght for intradermal delivery of vaccines. Vaccine 25 (34), 6423–6430.

Luboz, V., Chabanas, M., Swider, P., Payan, Y., 2005. Orbital and maxillofacial computer aided surgery: patient-specific finite element models to predict surgical outcomes. Comput. Methods Biomech. Biomed. Eng. 8 (4), 259–265.

Luboz, V., Promayon, E., Payan, Y., 2014. Linear elastic properties of the facial soft tissues using an aspiration device: towards patient specific characterization. Ann. Biomed. Eng. 42 (11), 2369–2378.

Luebberding, S., Krueger, N., Kerscher, M., 2014. Mechanical properties of human skin in vivo: a comparative evaluation in 300 men and women. Skin. Res. Technol. 20 (2), 127–135.

Maibach, H.I., 2002. Bioengineering of the skin. In: Elsner, P., Berardesca, E., Wilhelm, K., Maibach, H.I. (Eds.), Skin Biomechanics. CRC Press, Boca Raton, FL, USA Dermatology: Clinical & Basic Science Series.

Moiemen, N., Yarrow, J., Hodgson, E., Constantinides, J., Chipp, E., Oakley, H., Shale, E., Freeth, M., 2011. Long-term clinical and histological analysis of integra dermal regeneration template. Plast. Reconstr. Surg. 127 (3), 1149–1154.

Mollemans, W., Schutyser, F., Nadjmi, N., Maes, F., Suetens, P., 2007. Predicting soft tissue deformations for a maxillofacial surgery planning system: from computational strategies to a complete clinical validation. Med. Image Anal. 11 (3), 282–301.

Murray, B.C., Wickett, R.R., 1996. Sensitivity of cutometer data to stratum corneum hydration level. Skin Res. Technol. 2 (4), 167–172.

Pieper, S., Laub, D.R.J., Rosen, J.M., 1995. A finite-element facial model for simulating plastic surgery. Plast. Reconstr. Surg. 96 (5), 1100–1105.

Piérard, G.E., Nikkels-Tassoudji, N., Piérard-Franchimont, C., 1995. Influence of the test area on the mechanical properties of the skin. Dermatology 191, 9–15.

Piérard, G.E., Piérard, S., Delvenne, P., Piérard-Franchimont, C., 2013. In vivo evaluation of the skin tensile strength by the suction method: pilot study coping with hysteresis and creep extension. ISRN Dermatol. 2013, 1–7.

Rennekampff, H.-O., Rabbels, J., Reinhard, V., Becker, S.T., Schaller, H.-E., 2006. Comparing the Vancouver scar scale With the cutometer in the assessment of donor site wounds treated With various dressing in a randomized trial. J. Burn Care Res. 27 (3), 345–351.

de Rigal, J., Escoffier, C., Querleux, B., Faivre, B., Agache, P., Lévêque, J.-L., 1989. Assessment of aging of the human skin by in vivo ultrasonic imaging. J. Invest. Dermatol. 93 (5), 621–625.

Ryu, H.S., Joo, Y.H., Kim, S.O., Kyoung, C.P., Youn, S.W., 2008. Influence of age and regional differences on skin elasticity as measured by the cutometer(R). Skin. Res. Technol. 14 (3), 354–358.

Smalls, L.K., Wickett, R.R., Visscher, M.O., 2006. Effect of dermal thickness, tissue composition, and body site on skin biomechanical properties. Skin. Res. Technol. 12 (1), 43–49.

Staloff, I.A., Guan, E., Katz, S., Rafailovitch, M., Sokolov, A., Sokolov, S., 2008. An in vivo study of the mechanical properties of facial skin and influence of aging using digital image speckle correlation. Skin. Res. Technol. 14 (2), 127–134.

Takema, Y., Yorimoto, Y., Kawai, M., Imokawa, G., 1994. Age-related changes in the elastic properties and thickness of human facial skin. Br. J. Dermatol. 131 (5), 641–648.

Then, C., Stassem, B., Depta, K., Silber, G., 2017. New methodology for mechanical characterization of human superficial facial tissue anisotropic behaviour in vivo. J. Mech. Behav. Biomed. Mater. 71, 68–79.

van Zuijlen, P., van Trier, A., Vloemans, J., Groenevelt, F., Kreis, R., Esther, Middelkoop, 2000. Graft survival and effectiveness of dermal substitution in burns and reconstructive surgery in a one-stage grafting model. Plast. Reconstr. Surg. 106 (3), 615–623.

Vogt, M., Ermert, H., 2005. Development and evaluation of a high-frequency ultrasound-based system for in vivo strain imaging of the skin. IEEE Trans. Ultrason. Ferroelectr. Freq. Control 52, 375–385.

Wang, Y., Marshall, K.L., Baba, Y., Gerling, G.J., Lumpkin, E.A., 2013. Hyperelastic material properties of mouse skin under compression. PLoS ONE 8 (6), e67439-1 (e67439-9).
Weickenmeier, J., Jabareen, M., 2014. Elastic-viscoplastic modeling of soft biological tissues using a mixed finite element formulation based on the relative deformation gradient. Int. J. Numer. Methods Biomed. Eng. 30 (11), 1238–1262.
Weickenmeier, J., Jabareen, M., Mazza, E., 2015. Suction based mechanical characterization of superficial facial soft tissues. J. Biomech. 48 (16), 4279–4286.
Wortsman, X., Wortsman, J., Carreño, L., Morales, C., Sazunic, I., Jemec, G.B., 2013. Sonographic Anatomy of the Skin, Appendages, and Adjacent Structure in Dermatologic Ultrasound with Clinical and Histologic Correlations. Springer, New York, pp. 15–35.